· Article · Advances in Polar Science
doi: 10.13679/j.advps.2020.0007 June 2020 Vol. 31 No. 2: 92-102

Surface ozone variations at the Great Wall Station, Antarctica during austral summer

Justin SENTIAN[1*], Franky HERMAN[1], Mohd Sharul MOHD NADZIR[2] & Vivian Kong WAN YEE[1]

[1] Climate Change Research Group, Faculty of Science and Natural Resources, Universiti Malaysia Sabah, 88400 Kota Kinabalu, Sabah, Malaysia;
[2] Faculty of Science and Technology, Universiti Kebangsaan Malaysia, 43600 UKM Bangi, Selangor, Malaysia

Received 24 February 2020; accepted 25 May 2020; published online 15 June 2020

Abstract Surface ozone (O_3) is a secondary pollutant harmful to human health and a greenhouse gas which is one of the prime climate forcers. Due to the clean atmospheric environment of the Antarctic region and given the complexity of O_3 chemistry, the observation of surface O_3 variability in this region is necessary in the quest to better understand the potential sources and sink of polar surface O_3. In this paper, we highlighted our observations on O_3 variability at the Great Wall Station (GWS) during austral summer in December 2018 and January 2019. The continuous surface O_3 measurement at the GWS, Antarctica was carried out using the Ecotech Ozone analyzer. To understand the roles of the meteorological conditions on the temporal variations of O_3, meteorological data was obtained from the conventional auto-observational station at the GWS. The Hybrid Single-Particle Lagrangian Integrated Trajectory (HYSPLIT) model was employed to investigate the air mass transport over the region. The observed austral summer surface O_3 concentrations at the GWS exhibited variability and were significantly lower than those previously observed at other permanent coastal stations in Antarctica. The surface ozone variability at the GWS was strongly influenced by the synoptic change of air mass origin although the roles of photochemistry production and destruction were still uncertain. Marine characteristics and stable surface O_3 characterized the air masses that reached the GWS. The unique characteristic of surface O_3 at the coastal site of GWS was emphasized by its synoptic air mass characteristics, which displayed a significant influence on surface O_3 variability. Air mass that traveled over the ocean with relatively shorter distance was linked to the lower O_3 level, whereby the marine transport of reactive bromine (Br) species was thought to play a significant role in the tropospheric chemistry that leads to O_3 destruction. Meanwhile, the diurnal variation indicated that the O_3 background concentration levels were not strongly associated with the local atmospheric conditions.

Keywords **surface ozone, Great Wall Station, austral summer, HYSPLIT**

Citation: Sentian J, Herman F, Mohd Nadzir M S, et al. Surface ozone variations at the Great Wall Station, Antarctica during austral summer. Adv Polar Sci, 2020, 31(2): 92-102, doi: 10.13679/j.advps.2020.0007

1 Introduction

Among all greenhouse gases (GHGs), surface ozone (O_3) is considered as the most important because it plays a dual role depending on where in the atmospheric layers it resides. O_3 in both the stratosphere and troposphere has a critical role in atmospheric chemistry. Tropospheric O_3 is considered a pollutant and a GHG. Unlike other well-mixed GHGs, tropospheric O_3 exhibits spatial and temporal inhomogeneous distribution (Sudo and Akimoto, 2007) and is acknowledged as one of the key factors in controlling global-scale climate change and air quality (Mickley et al.,

* Corresponding author, ORCID: 0000-0002-7121-2372, E-mail: jsentian@ums.edu.my

2004; Gauss et al., 2006). However, it has also been found to be essential in driving gas-phase chemistry and initiating oxidation of reduced compounds, thus cleansing the atmosphere of a wide range of pollutants (Monks et al., 2015; Schultz et al., 2015).

In the stratosphere, O_3 acts as a regulator filtering harmful ultraviolet radiations, particularly ultraviolet B (UVB) and ultraviolet C (UBC) from reaching the earth's surface and causing a deleterious impact on life on earth (Lucas, 2011). The thin O_3 layer in the lower stratosphere is enriched with a high concentration of O_3 thus shielding life on earth from harmful UV radiation. The stratospheric O_3 is relatively dry and stable, and thus inhibits a mixture of gases between the stratosphere and the troposphere which ultimately maintains the atmospheric composition between the respective atmospheric layers (Mihalikova et al., 2012).

There is great research interest on the spatial and temporal variations of surface O_3 at the polar region, which is dynamically regulated by the sources as well as the local and regional meteorological conditions. At the polar region, the main source of surface O_3 is the production of photochemical reactions involving its precursors such as NO_x and VOCs. Another source, which remains uncertain, is the natural atmospheric influx process from the stratosphere through a mechanism known as stratosphere–troposphere transport (STT) (Greenslade et al., 2017; Tarasick et al., 2019). A previous study reported that the elevated surface O_3 at the polar region was sometimes associated with air mass transport within the region and photochemically produced at lower latitude (Legrand et al., 2016).

Previous *in-situ* measurements of surface O_3 over the Antarctic region had documented distinct seasonal changes, which maximize during winter and minimize during summer (Cristofanelli et al., 2011; Legrand et al., 2016; Nadzir et al., 2018). Investigations of surface O_3 variability over the Antarctic region at different temporal and geographical scales had highlighted surface O_3 characteristics and factors that may be responsible for the surface O_3 background. It is generally believed that surface O_3 variability at the Antarctic region is a result of a complex interaction between the dynamic atmosphere characteristics and the topographical setting. In addition, the region's high sensitivity to global temperature changes may also contribute to the surface ozone variability, although the efforts in understanding the atmospheric feedback processes in climate-related studies is actively progressing (Neff et al., 2008). The scarcity of anthropogenic source and sink of O_3 in this region further complicates the current understanding of O_3 variability.

Limited studies on surface O_3 in Antarctica warrants a research approach that aims to understand the characteristics of surface O_3 background and to provide any additional information about ozone dynamics in the polar region. The main objective of this study is to report the observed surface O_3 variability during austral summer at the Great Wall Station (GWS) on the slopes of King George Island, Antarctica. The evaluation was made by comparing the results of this study with other previous measurements at various research stations. In this paper, we also described the local and regional meteorological conditions (temperature, atmospheric pressure, humidity, radiation exposure and surface wind) and investigated the role of air mass transport on the surface O_3 characteristics.

2 Measurement site and method

The GWS is located on the western side of the Antarctic Peninsula (Figure 1). The austral summer campaign of surface O_3 measurement began on 20 December 2018 and ended on

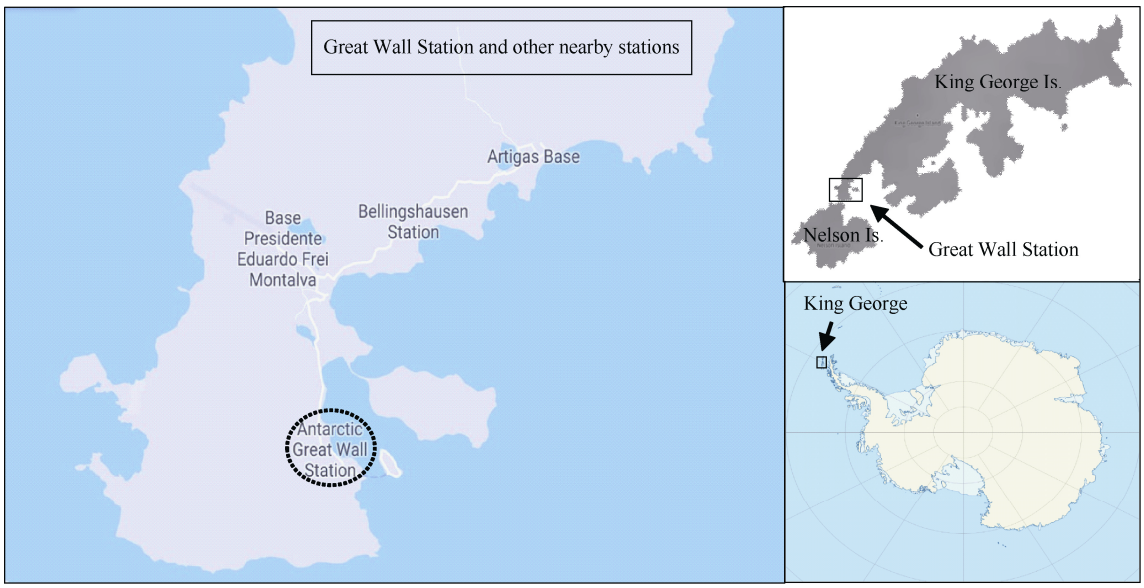

Figure 1 Location of the austral summer O_3 measurement at the GWS on the western side of the Antarctic Peninsula.

15 January 2019. An Ecotech Serinus O_3 analyzer was used to measure the surface O_3 throughout the course of the campaign. The Ecotech O_3 analyzer was calibrated twice based on a seven-point standard O_3 sample (ranging from very low to very high concentration). The first calibration was made to check the precision of the analyzer prior to the austral summer campaign. The second calibration was made after the campaign to check for any drifting of the calibration curve. The calibration of the instrument follows the standard calibration procedure of the manufacturer (EC9811-Ozone Analyser User Manual). The calibration procedure principle is based on the photometric analysis of ozone concentrations in a dynamic flow system. The concentration of ozone in the absorption cell is determined by the measurement of the amount of 254 nm light absorbed by the sample. The multipoint calibration consists of seven (7) concentrations across the instruments operating in a range of 0.1 to 200 ppbv (parts per billion by volume). The concentration levels are derived to determine the accuracy between the calculated and expected values of the analyser using a simple Excel spreadsheet analysis. Based on the standard operation manual, the calibration is accepted if the gradient (measured vs calculated plot) falls between 0.98 and 1.02; the intercept of the trendline lies between −0.3 and 0.3; and the correlation (R^2) is greater than 0.9995. The instrument detection limit is 0 to 50 ppb with an accuracy or precision of 0.5 ppb or 0.2%. The multipoint calibration plot is shown in Figure 2. The same calibration procedure was used for the same instrument in our previous study in Antarctica as mentioned in Nadzir et al. (2018).

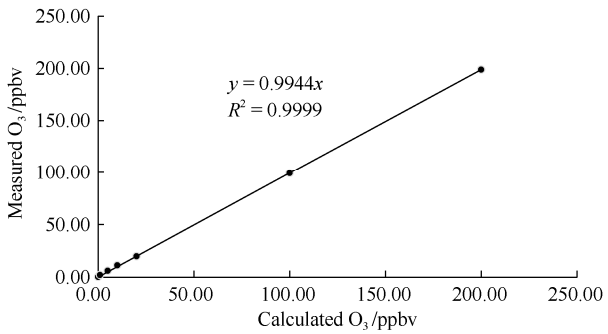

Figure 2 Ecotech ozone analyser: multipoint calibration plot.

Real-time O_3 measurement was carried out continuously at the GWS for 32 d with a sampling frequency of 10-min intervals. The instrument was located upwind of the station to minimize contamination from potential local sources emissions. The inlet of the sampling line of the O_3 analyzer was located at 3 m above ground level by using a Teflon sample line with a diameter of 0.25 cm, which was adjusted to face the prevailing wind for better air channeling. The O_3 analyzer and the sampling line input were inspected regularly using the Meteorological parameters such as temperature, atmospheric pressure, humidity, total radiation exposure and surface wind which were recorded by the automatic weather station (AWS) operating at the GWS. The available instruments included a thermocouple (for surface temperature), piezoelectric sensor (for atmospheric pressure), capacitor device (for relative humidity) and an anemometer (for surface wind speed and direction measurement). Meteorological data was recorded at 25 m above snow surface for every minute and validated at 1-h intervals for data processing.

3 Trajectory analysis

To analyze the regional air mass transport over the Antarctic Peninsula, the air mass history of the atmosphere was simulated using backward trajectory analysis. A 5-d (120 h) backward trajectory was computed from 00:00, 06:00, 12:00, and 18:00 UTC at 500 m A.G.L from each sampling. The back trajectories and horizontal dispersion clustering were calculated using version 4.9 of the Hybrid Single Particle Lagrangian Integrated Trajectory (HYSPLIT) model developed by the National Oceanic and Atmospheric Administration (NOAA)'s Air Resource Laboratory (ARL) which is available at http://ready.arl.noaa.gov/HYSPLIT.php. The meteorological data from the Global Data Assimilation Process was used as input for the model and is available at ftp://arlftp.arlhq.noaa.gov/pub/archieves. HYSPLIT provides a complete, complex and efficient application that can be used to compute simple trajectories, dispersion, and deposition simulations under a given meteorological setting and has been recognized as the most used backward trajectories model application (Draxler, 1999).

The model utilizes a moving frame of reference for the advection and diffusion calculation and a fixed 3D grid frame to compute pollutant concentrations (Stein et al., 2015). In this study, a 5-d backward trajectory analysis on a selected period with 3 points of elevation above mean sea levels (AMSL) of 0 m, 100 m, and 500 m with a 6-h interval starting at 00:00 local time was carried out. The backward trajectories analysis did not provide any information pertaining to surface O_3 such as the mixing ratio, dispersion or chemistry, but it did provide information about the air mass path into the observation station and estimation of the potential source at a particular point of time.

4 Results and discussion

4.1 Background meteorological conditions

Continuous meteorological data such as atmospheric temperature, pressure, humidity, radiation exposure, wind speed, and wind direction were recorded by the AWS operating at GWS. For most of the days, the hourly surface temperature increased until 16:00 and decreased afterwards. The temperature varies greatly from −1.4 ℃ to 5.9 ℃.

Meanwhile, the atmospheric pressure did not show much noticeable variations, with pressure ranging from 965.8 hPa to 995.6 hPa. For each of the days, fluctuating hourly humidity with variations from 58% to the highest value of 97% were observed. The radiation exposure varies from 0 $MJ{\cdot}m^{-2}$ to 3.23 $MJ{\cdot}m^{-2}$. Zero radiation exposure was recorded for the first 2 h of measurement before it began to increase until 13:00 and decreased afterwards before eventually returning to zero. Meanwhile, the prevailing winds were characterized by low speeds of 3 $m{\cdot}s^{-1}$ to 10 $m{\cdot}s^{-1}$, blowing from a westerly direction. The highest wind speeds were between 15 $m{\cdot}s^{-1}$ and 17.5 $m{\cdot}s^{-1}$ from an easterly direction.

4.2 Temporal characterization of surface O_3 observation

The daily mean surface O_3 concentration at GWS were between 5.37 ppbv and 5.57 ppbv with average daily changes of between −0.03 ppbv and +0.02 ppbv. The standard deviation of the O_3 dataset was 0.056. This indicates that the daily surface O_3 variations were quite stable during the whole period of measurement. However, the time-series data depicts an hourly fluctuating O_3 concentration, where the daily and hourly means of O_3 were observed to be between 4.45 ppbv and 7.81 ppbv (Figure 3). The fourth day of observation marked the highest hourly concentration with 7.81 ppbv (with a sudden maximum increase of 2.60 ppbv) observed at 04:00. The lower concentrations were observed on 20, 30 and 31 December 2018 where the O_3 concentration decreased between 4.45 ppbv and 4.49 ppbv (with sudden decreases by 1.18 ppbv, 1.06 ppbv, and 0.84 ppbv respectively), at 12:00, 08:00 and 20:00 respectively. Meanwhile, throughout the rest of December 2018 and January 2019, the hourly concentrations of O_3 fluctuated between 0.50 ppbv and 0.84 ppbv. This characteristic suggests that the sudden net of production and loss of surface O_3 can be linked to the synoptic conditions and photochemistry reactions under a low NO_x regime as pointed out previously by Cristofanelli et al. (2018) and Legrand et al. (2009, 2016).

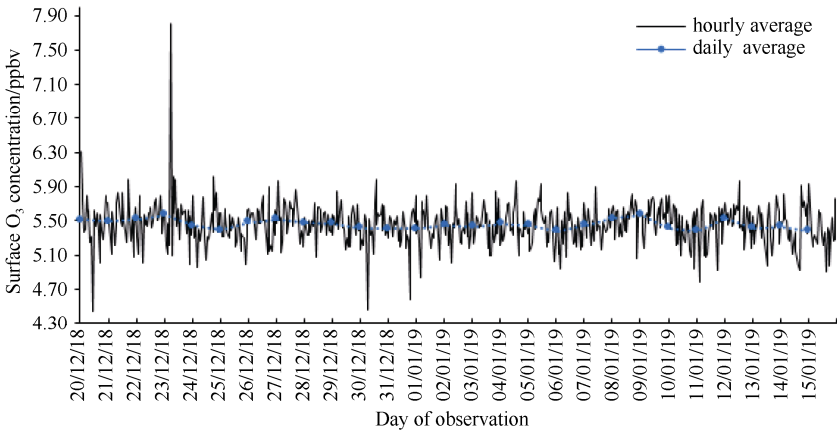

Figure 3 Hourly (black line) and daily (blue dot) surface O_3 average concentrations at GWS during the austral summer measurement campaign.

4.3 Role of air mass transport

The preceding discussion of Crawford et al. (2001), Frey et al. (2005) and Legrand et al. (2009) suggested that air mass transport can greatly affect the background of the measured O_3 levels, although the effects are temporary in nature. These transport condition can be either favourable to the production of O_3 accumulation or unfavourable, depending on whether a greater proportion of its time is spent first over the free tropospheric latitudes, inland and Antarctic Plateau, outside the Antarctic continent and over the coastal and marine boundary layer. To this extent, the backward trajectory analysis could provide a substantial explanation of the surface O_3 characteristics. In this study, four clusters of the 5-d backward trajectories (Figure 4) were generated to assess the origins and possible influence of the synoptic air mass transport to the surface O_3 background level at GWS.

The backward trajectories analysis led to the identification of four patterns of air mass transport with a similar air mass origin, but with different compositions of marine events. Overall, the air mass arriving at the measurement site as shown in Figure 4 can be assumed to be representative of the marine boundary layer. The air masses arriving at GWS could have originated 1200–6200 km away from the South Pacific Ocean (SPO) and Southern Ocean (SO) before arriving at the measurement site. As depicted in Figure 4a and Figure 4c, despite the almost similar air mass transport characteristics observed over the ocean, the measured O_3 levels were relatively varied and slightly higher during the first week of measurement. During the first five days (Figure 4a: 20–24 December 2018), 95%–98% of the air mass originating from the SPO and SO/Bellingshausen Sea had travelled over the ocean with a trajectory length of between 3600–6000 km

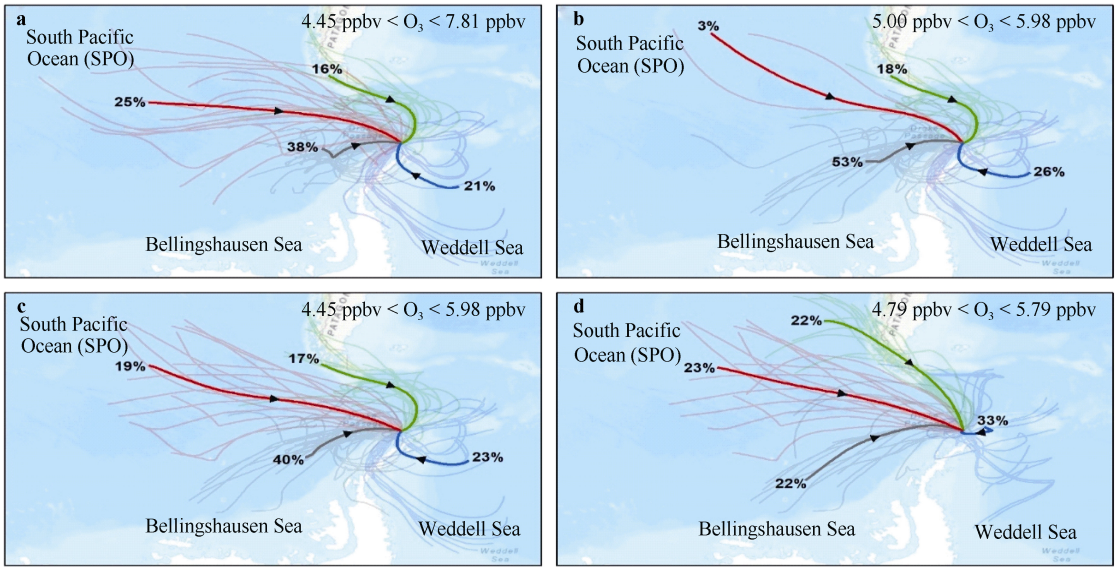

Figure 4 The 5-d backward trajectories and relative O_3 hourly concentration starting from: **a**, 24 December 2018; **b**, 29 December 2018; **c**, 2 January 2019; **d**, 13 January 2019.

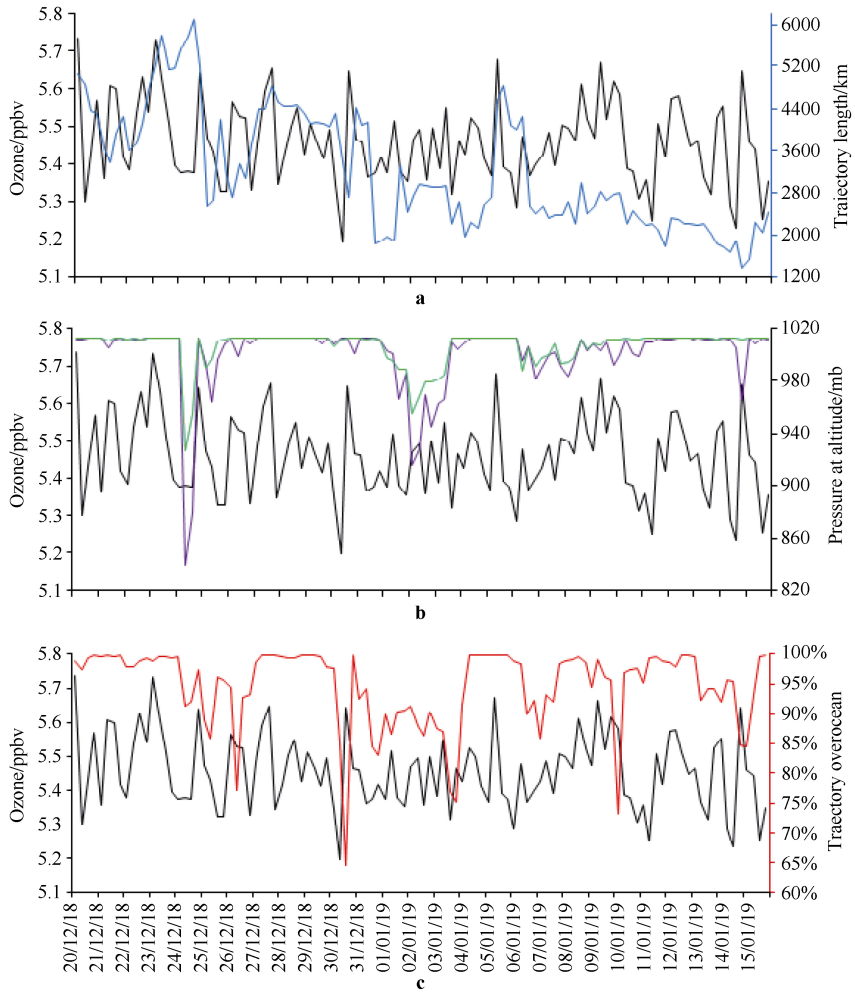

Figure 5 The 6-h average O_3 and the corresponding 5-d backward trajectories analysis at GWS. The black line represents the 6-h average O_3. The blue line in (**a**) shows the trajectory length, while the purple and green line in (**b**) represents the average altitude in pressure of air masses at 5-d and 3-d prior its arrival, the red line in (**c**) shows the residence time fraction of air masses prior to their arrival at GWS.

(Figure 5a), indicating that air masses travelling over the SPO were relatively enriched with O_3. At the end of December 2018 and early January 2019 (Figure 4c), the hourly O_3 variability was relatively less whilst the air mass trajectory was characterized with shorter lengths (1800–4500 km) with less frequency of air mass originating from SPO and less fraction spent of air mass over the ocean (65%–98%). In a previous study, the depletion of O_3 was reported to be linked to the marine transport of reactive bromine (Br) species, which has a major role in tropospheric chemistry that leads to O_3 destruction (Spicer et al., 2002; Avallone et al., 2003). However, since the lifetime of reactive Br species is relatively short (less than half day), the effective role of Br in the tropospheric reactions from the marine transport is limited from the direct vicinity of the measurement site (Avallone et al., 2003). This is reflected well at our GWS measurement, in which more O_3 destruction was observed as the air mass originated from the Bellingshausen Sea and Weddell Sea. The air masses from these regions may contain either O_3 depleted air or rich in residual gas-phase halogen species such as Br.

Analysis on the 6-h averaged O_3, air mass trajectories and the total fraction time spent by the air masses over the ocean suggested that longer trajectories (>3500 km) were generally associated with highly varied and comparatively higher O_3 levels. For example, the O_3 background level observed from 20 to 24 December 2018 (Figure 4a) recorded an hourly concentration of between 4.45 ppbv to 7.81 ppbv. During this time, the 6-h O_3 level was generally enhanced as the air mass travelled longer over the ocean (Figure 5a) with a high fraction time spent by the air mass over the ocean (Figure 5b). Further analysis on the vertical evolution of the trajectory showed that 87% of the trajectory time was spent within the marine boundary layer (about 992 mb or about 200 m). Within the marine boundary layer, 63% of the trajectory time was spent below 50 m. This suggests that the air mass was largely confined within the marine boundary layer. Long trajectory indicates that the origin of the air mass that arrived at GWS was relatively far, and therefore allows for the accumulation of O_3 or its precursor prior to its arrival at the measurement site thus favouring O_3 production. Statistical analysis was also performed to determine if there are any relationships between air mass with the synoptic ozone level for the 5-d and 3-d trajectories. The results showed that there are positive correlations (significance level alpha=10%; *p*-value=0.075) between the average ozone level with the trajectory length. The average ozone levels also showed negative correlations with the air mass trajectory heights (both 5-d and 3-d). These could suggest that the synoptic surface ozone variations were substantially influenced by the length of the air mass travelled and the air mass travelled height within the marine boundary layer. This carries the expectation that the dynamics of the lower atmosphere at the GWS and the nature of its surroundings could be the main player controlling the surface O_3 background level.

It was also observed that low 6-h averaged O_3 was not necessarily associated with short trajectories, which indicates lower time fraction spent over the ocean (Figure 5c), but also depending on the effective marine transport of important reactive halogenated species. The presence of BrO and Br ozone is lost through the catalytic reactions. The effective marine transport of halogenated species is characterized by closer emission sources to the vicinity of the measurement site, having travelled below 100 m height with significant amount of time over the sea surface (Frieβ et al., 2004). Under this condition, it is perceived that the air mass would be stable and well mixed, and able to uptake reactive halogenated species from the sea surface. Sudden decreases of O_3 levels were observed towards the end of December 2018 (30 and 31 December 2018). During this period, the air mass travelled over the ocean and spent relatively less time fraction over the ocean as compared to during the first week of measurement. Extreme concentrations of halogenated species especially Br in Weddell Sea region as reported by Riedel (2005) could play an important role in the sudden decreases of the O_3 concentrations. As for the O_3 depletion event observed on 20 December 2018, no obvious source of reactive Br near the vicinity of measurement site could be identified. Based on a previous study (Tarasick and Bottenheim, 2002), there was also considerable evidence that O_3 depletion was also observed during the long transport of air mass. Spatial and temporal variations of the zonal total column of BrO ($mol \cdot mol^{-1}$) in the surrounding region of the Antarctic Peninsula as retrieved from the MLS-AURA satellite between January 2018 and January 2019 (Figure 6) has shown variability. Seasonally, the BrO concentrations over the Antarctic Peninsula (surrounding the regions of King George Island–SO/Bellingshausen Sea & Weddell Sea) were in the ranges of -1.6×10^{-11} – 3.0×10^{-11} $mol \cdot mol^{-1}$ (Summer: Dec 18–Feb 19); -0.8×10^{-11} – 4×10^{-11} $mol \cdot mol^{-1}$ (Autumn: Mar 18–May 18); -1.0×10^{-11} – 4×10^{-11} $mol \cdot mol^{-1}$ (Winter: Jun 18–Aug 18); and -0.5×10^{-11} – 3.5×10^{-11} $mol \cdot mol^{-1}$ (Spring: Sept 18–Nov 18). The monthly and seasonal BrO distributions over the region were observed to be fluctuating within the same range. As such, the significance of the O_3 loss due to Br chemistry warrants further investigation, which includes the incorporation of a detailed Br chemistry scheme into the tropospheric chemical transport model. In comparison, the O_3 enhancement in the southern polar region, particularly on the eastern part of the Antarctic continent during austral summer, has been widely reported (Crawford et al., 2001; Kumar et al., 2007; Helmig et al., 2007, 2008; Legrand et al., 2016; Cristofanelli et al., 2018) and the O_3 enhancement was linked to the air mass transport from the Antarctic Plateau or from a lower latitude, and photo-denitrification of the summer snowpack, resulting in NO_x emissions to the atmosphere responsible for the surface O_3 variability

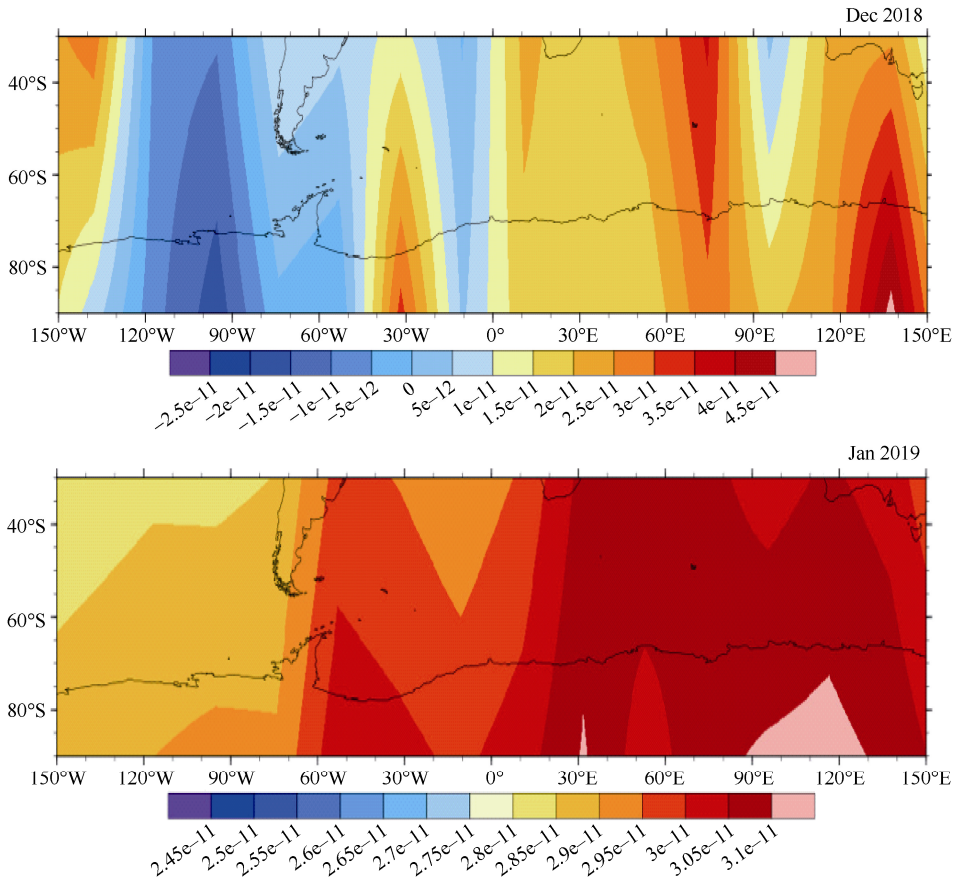

Figure 6 Spatial and temporal analysis of BrO zonal total column (mol·mol^{-1}) retrieve from MLS-AURA satellite over Antarctic Peninsula and its surrounding from December 2018 to January 2019.

through photochemical reactions (Jones et al., 1999; Jones et al., 2000; Jones et al., 2001; Jones et al., 2008).

4.4 Diurnal characteristic of surface O_3 at GWS

To illustrate the potential surface O_3 diurnal trends at GWS, the calculated daily mean and the hourly variation for the few selected days over which the O_3 level patterns were highly variant and most invariant throughout the observation period were examined. During the measurement campaign, there was no clear diurnal cycle at GWS. Further examination of the relationships between ozone maxima, minima and meteorological was carried out to provide an important measure of confidence on the roles of the meteorological factors on O_3 diurnal variability during austral summer. Based on the selected 4 d, the overall trends showed a non-clear or non-significant relationship with the local meteorological conditions (Figure 5) although the sudden increase of O_3 observed on 23 December 2018 at 05:00 LT that coincided with a stable synoptic weather condition (wind speed) may be noteworthy. Meanwhile, during the unstable synoptic weather conditions, the surface O_3 variability was found to be less varied, and on some occasions, sudden decreases of O_3 were also observed (Figure 7a–7d). During this particular period, the meteorological conditions might not be favorable for the photochemistry production of O_3 or might have been offset by either the low or high halogen and radical species, or O_3 precursors that travelled along the trajectory especially those closer to the measurement site. It is also suggested that the external effect that influences surface O_3 variability was time-variant, and the potential of O_3 photochemical processes occurring in the atmosphere is temporally variable. A much earlier study (Galbally and Allison, 1972) suggested that O_3 variability was possibly influenced by the variabilitity of O_3 fluxes over the few days old surface snow which could also explain the results of this study, although this warrants further investigation.

The air mass travelling into GWS, which is generally driven by meteorological factors as reported elsewhere over the Antarctica region (Monks, 2000; Legrand et al., 2009; Cristofenelli et al., 2011) may exert significant impact to O_3 diurnal variability. The distribution differences in wind frequencies and wind speeds may have significant impacts on the reduction and advection of O_3. As depicted in Figure 7d and 7h, the wind direction is rather unstable under lower wind speed conditions, and therefore demonstrated an unfavorable condition for pollutant diffusion as mentioned previously in (Oltmas et al., 2008;

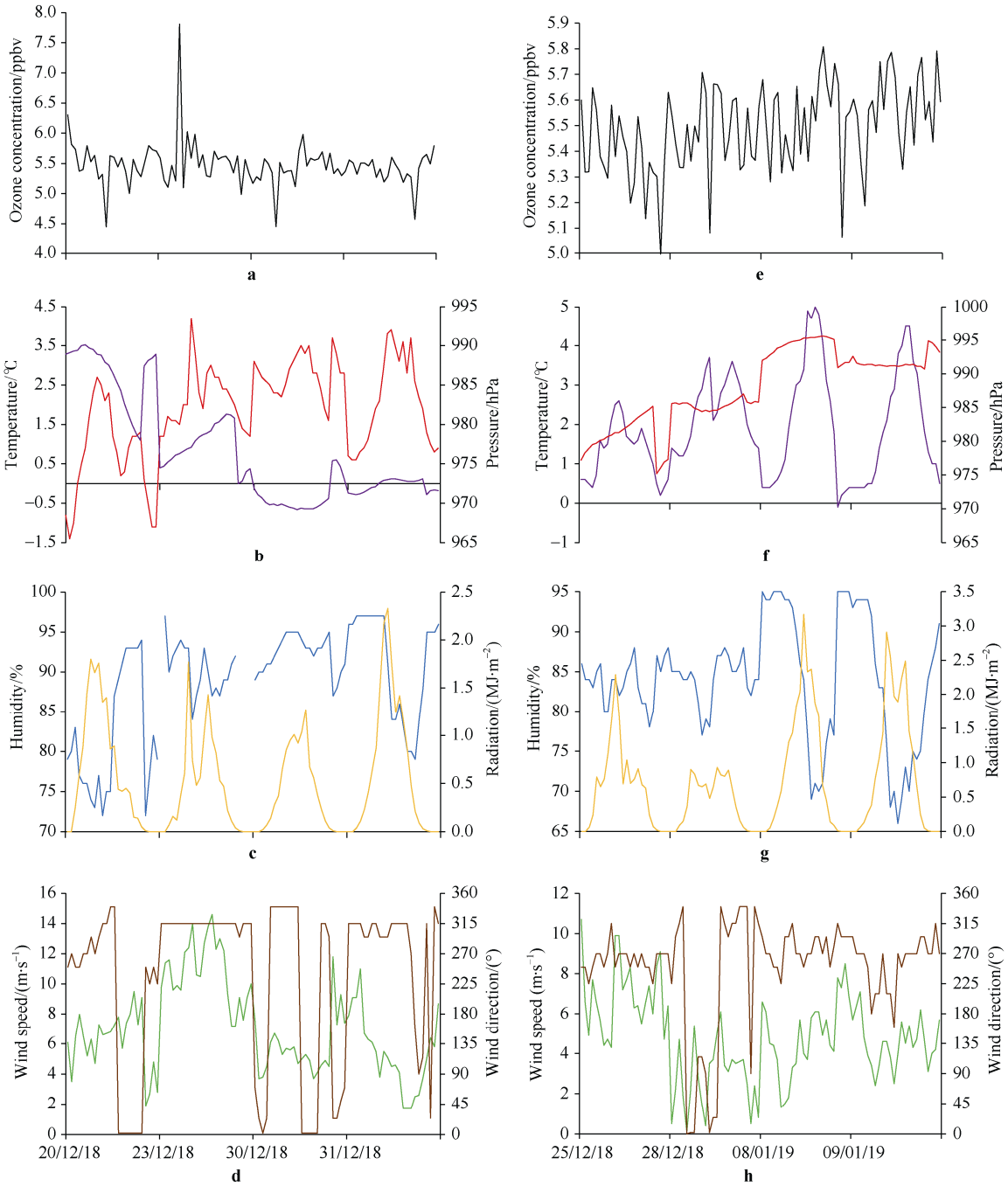

Figure 7 Hourly averaged surface O_3 concentration together with weather conditions during the most variant surface O_3 concentration (**a**–**d**), and the most stable O_3 concentration (**e**–**h**). The black line represents O_3 concentration, the red line represents temperature, the purple line represents atmospheric pressure, the blue line represents humidity level, the yellow line represents radiation, while the green and brown lines represent wind speed and its direction.

Wang et al., 2011; Ali et al., 2017; Bian et al., 2018). Therefore, we cannot rule out that the surface O3 concentration may change with the increase of wind speed, which is responsible for the atmospheric dilution and dispersion, and hence the decrease of O_3 background concentration. Thus, the interpretation of the meteorological factors on the surface O_3 concentration variations requires understanding of their surrogate impact rather than a singular visualization of the meteorological parameter.

A better visualization of the relationship between the O_3 variation and the surrogate impact of the meteorological parameters is depicted in Figure 7e–7h. It can be observed that on 28 December 2018 from 05:00 to 10:00 of LT, the atmospheric pressure almost remained unchanged (fluctuated between 984.5 hPa and 984.9 hPa) (Figure 7f), the temperature was above 2.0 ℃ (Figure 7f) with a

decreasing humidity level (Figure 7g), and a wind speed lower than 6 $m \cdot s^{-1}$ (Figure 7h). This condition should be favorable for the photochemical production of O_3; however, the O_3 level was only observed to increase slightly from 5.36 ppbv to 5.71 ppbv. Further, the increase of O_3 is not prominent as it has been offset by the changing wind speed and direction at 10:00 LT. A similar scenario was observed between 11:00 to 13:00 LT, where the O_3 level remained around 5.66 ppbv and decreased once again when the wind speed and wind direction changed. On the same day, between 14:00 and 20:00 LT, the wind speed was calm and blowing approximately from the same direction with a temperature above 2.0 ℃ and small changes in humidity (less than 2%). At this point, the O_3 level increased from 5.36 ppbv to 5.61 ppbv with an increasing pressure level from 985.2 hPa to 986.8 hPa. However, the O_3 level decreased soon after the atmospheric pressure reached higher than 987 hPa at 18:00 LT. Therefore, changes in atmospheric pressure may be indicative of O_3 changes but in areas that are almost free from any direct anthropogenic precursors for ozone photochemical local production or destruction, the dynamical process for ozone should be obvious.

To further evaluate the influence of these meteorological factors on surface O_3 level during the most invariant and variant O_3 level, a statistical principal component analysis (PCA) was performed. The results of both cases indicated that three factors have eigenvalues cut-off at unity 70% (with total variance explained of about 70% by these three factors). The strengths of the dependency of O_3 in both cases are shown in Table 1. During the most variant O_3 in factor 1, it was found that only atmospheric pressure was important in influencing O_3 production. Meanwhile in factor 2, it was found that O_3 was not appreciably influenced by both temperature and solar radiation. However, in factor 3, wind speed was found to be more effective in influencing diurnal surface O_3 compared to the atmospheric pressure system in factor 1. In factor 3, apart from the wind speed, wind direction was also found to be influential to the surface O_3 variability. Therefore, this observation suggests that the high diurnal variability of O_3 was significantly influenced by changes in the atmospheric pressure system and surface wind profile. Meanwhile, the PCA analysis during invariant O_3 reveals that in factor 1, surface temperature was strongly associated with the diurnal O_3 variability followed by radiation and atmospheric pressure. In factor 2, wind speed significantly influenced the diurnal O_3 variability followed by radiation and temperature. Meanwhile in factor 3, wind direction and wind speed were the most associated with the diurnal O_3 variability. Thus, under the presence of a stable lower atmospheric layer, the change of wind speed and wind direction can still cause a residual change of lower atmospheric O_3 level due to the dispersion or the transport of O_3 and other species into the regime.

Table 1 PCA results for O_3 and the meteorological parameters for GWS

Components	Most variant O_3			Invariant O_3		
	Factor 1	Factor 2	Factor 3	Factor 1	Factor 2	Factor 3
Ozone/ppbv	0.171	0.245	0.405	0.282	−0.435	0.064
Temperature/℃	−0.420	−0.516	−0.071	0.563	0.156	0.069
Pressure/hPa	0.667	−0.022	0.048	0.265	−0.663	0.144
Humidity/%	−0.571	0.268	0.275	−0.497	−0.337	−0.022
Radiation/($MJ \cdot m^{-2}$)	0.069	−0.695	0.069	0.494	0.182	0.162
Wind speed/($m \cdot s^{-1}$)	−0.057	0.019	0.701	−0.179	0.389	0.619
Wind direction/(°)	0.120	−0.344	0.506	−0.101	−0.220	0.748
Eigenvalue	2.01	1.57	1.28	2.53	1.31	1.23
Variance explained/%	28.7	22.4	17.3	36.1	18.7	17.5
Cumulative variance explained/%	28.7	51.1	69.4	36.1	54.8	72.3

5 Concluding remarks

The observed austral summer surface O_3 concentrations at GWS exhibit variability and are significantly lower than those previously observed at other permanent coastal stations in Antarctica. With the exception of a sudden O_3 increment on 23 December 2019 at 04:00 to 06:00 LT, the overall surface O_3 at GWS may be considered as homogeneity. Surface ozone variability at GWS was strongly influenced by the synoptic change of air mass origin although the roles of photochemistry production and destruction were still uncertain. Further, based on the backward trajectory analysis, the air masses reached at GWS were characterized by marine characteristic and stable surface O_3 indicating that air mass has a low O_3 background regime. Air mass that travelled over the ocean with relatively short distances (2800–4500 km) was linked to the lower O_3 level, which in turn was linked to the marine transport of reactive Br species that plays a major role in tropospheric chemistry leading to O_3 destruction.

Meanwhile, the diurnal variation indicated that the O_3 background concentration levels were not strongly

associated with the local atmospheric conditions. The unique characteristic of surface O_3 at the coastal site of GWS was emphasized by its synoptic air mass characteristics, which displayed significant influence on surface O_3 variability or rather increasing the photochemical activity given the availability of the precursors. On the other hand, the increase of surface wind speed was also found responsible for changes in surface O_3 concentration, either through the promotion of the distribution of O_3 precursors or through the transport of locally produced O_3 to the measurement station.

Acknowledgments This study was funded by the Sultan Mizan Antarctic Research Foundation (YPASM, 2017) Malaysia and supported by the Chinese Arctic and Antarctic Administration (CAA). We gratefully acknowledged the support by Universiti Malaysia Sabah (UMS) and especially for the staff at the Chinese Great Wall Station, Antarctica, during austral summer 2018/2019. The authors thank two anonymous reviewers for their construtive comments and suggestions.

References

Ali K, Trivedi D K, Sahu S K. 2017. Surface ozone characterization at Larsemann Hilss and Maitri, Antarctica. Sci Total Environ, 584-585: 1130-1137, doi: 10.1016/j.scitotenv.2017.01.173.

Avallone L M, Toohey D W, Fortin T J, et al. 2003. In situ measurements of bromine oxide at two high-latitudes boundary layer sites: implications of variability. J Geophys Res, 108: D34089, doi: 10.1029/2002JD002843.

Bian L G, Ye L, Ding M H, et al. 2018. Surface ozone monitoring and background concentration at Zhongshan Station, Antarctica. Atmos Clim Sci, 8(1): 1-14, doi: 10.4236/acs.2018.81001.

Crawford J H, Davis D D, Chen G, et al. 2001. Evidence for photochemical production of ozone at the South Pole surface. Geophys Res Lett, 28: 3641-3644, doi: 10.1029/2001GL013055.

Cristofanelli P, Calzolari F, Bonafè U, et al. 2011. Five-year analysis of background carbon dioxide and ozone variations during summer seasons at the Mario Zucchelli Station (Antarctica). Tellus B, 63(5): 831-842.

Cristofanelli P, Putero D, Bonasoni P, et al. 2018. Analysis of multi-year near-surface ozone observations at the WMO/GAW "Concordia" station (75° 06′S, 123° 20′E, 3280 m a.s.l – Antarctica). Atmos Environ, 177: 54-63, doi: 10.1016/j.atmosenv.2018.01.007.

Draxler R R. 1999. HYSPLIT4 user's guide. NOAA Tech. Memo. ERL ARL-230, NOAA Air Resources Laboratory, Silver Spring, MD.

Frey M M, Stewart R W, McConnell J R, et al. 2005. Atmospheric hydroperoxides in West Antarctica: Links to stratospheric ozone and atmospheric oxidation capacity. J Geophys Res, 110: D23301, doi: 10.1029/2005JD006110.

Frieβ U, Hollwedel J, König-Langlo G, et al. 2004. Dynamics and chemistry of tropospheric bromine explosion events in the Antarctic coastal region. J Geophys Res, 109: D06305, doi: 10.1029/2003 JD004133

Galbally I, Allison I. 1972. Ozone fluxes over snow surfaces. J Geophys Res, 77(21): 3946-3949.

Gauss M, Myhre G, Isaksen I S A, et al. 2006. Radiative forcing since preindustrial times due to ozone change in the troposphere and the lower stratosphere. Atmos Chem Phys, 6: 575-599, doi: 10.5194/acp-6-575-2006.

Greenslade J W, Alexander S P, Schofield R, et al. 2017. Stratospheric ozone intrusion events and their impacts on tropospheric ozone in the Southern Hemisphere. Atmos Chem Phys, 17: 10269-10290, doi: 10.5194/acp-17-10269-2017.

Helmig D, Johnson B, Oltmans S, et al. 2008. Elevated ozone in the boundary layer at South Pole. Atmos Environ, 42: 2788-2803, doi: 10.1016/j.atmosenv.2006.12.032.

Helmig D, Oltmans S J, Carlson D, et al. 2007. A review of surface ozone in the polar regions. Atmos Environ, 41: 5138-5161, doi: 10.1016/j.atmosenv.2006.09.053.

Jones A E, Weller R, Anderson P S, et al. 2001. Measurements of NO_x emissions from the Antarctic snowpack. Geophys Res Lett, 28: 1499-1502, doi: 10.1029/2000GL011956.

Jones A E, Weller R, Minikin A, et al. 1999. Oxidized nitrogen chemistry and speciation in the Antarctic troposphere. J Geophys Res, 104: 21355-21366, doi: 10.1029/1999JD900362.

Jones A E, Weller R, Wolff E W, et al. 2000. Speciation and rate of photochemical NO and NO_2 production in Antarctic snow. Geophys Res Lett, 27: 345-348, doi: 10.1029/1999GL010885.

Jones A E, Wolff E W, Salmon R A, et al. 2008. Chemistry of the Antarctic boundary layer and the interface with snow: an overview of the CHABLIS campaign. Atmos Chem Phys, 8: 3789-3803, doi: 10.5194/acp-8-3789-2008.

Kumar A, Gupta V B, Jain S, et al. 2007. Surface ozone variability between two different Antarctic sites. Indian J Radio Space Phys, 36: 59-64.

Legrand M, Preunkert S, Jourdain B, et al. 2009. Year-round record of surface ozone at coastal (Dumont d'Urville) and inland (Concordia) sites in East Antarctica. J Geophys Res, 114: D20306, doi: 10.1029/2008JD011667.

Legrand M, Preunkert S, Savarino J, et al. 2016. Inter-annual variability of surface ozone at coastal (Dumont d'Urville, 2004–2014) and inland (Concordia, 2007–2014) sites in East Antarctica. Atmos Chem Phys, 16: 8053-8069, doi: 10.5194/acp-16-8053-2016.

Lucas R M. 2011. An epidemiological perspective of ultraviolet exposure—public health concerns. Eye & Contact Lens: Sci Clinical Prac, 37(4): 168-175, doi: 10.1097/ICL.0b013e31821cb0cf.

Mickley L J, Jacob D J, Field B D, et al. 2004. Effects of future climate change on regional air pollution episodes in the United States. Geophys Res Lett, 31: L24103, doi: 10.1029/2004GL021216.

Mihalikova M, Kirkwood S, Arnault J, et al. 2012. Observation of a tropopause fold by MARA VHF wind-profiler radar and ozonesonde at Wasa, Antarctica: comparison with ECMWF analysis and a WRF model simulation. Ann Geophys, 30(9): 1411-1421, doi: 10.5194/ angeo-30-1411-2012.

Monks P S. 2000. A review of the observation and origins of the spring ozone maximum. Atmos Environ, 34: 3545-3561.

Monks P S, Archibald A T, Colette A, et al. 2015. Tropospheric ozone and its precursors from the urban to the global scale from air quality to short-lived climate forcer. Atmos Chem Phys, 15: 8889-8973, doi: 10.5194/acp-15-8889-2015.

Nadzir M S M, Ashfold M J, Khan M F, et al. 2018. Spatial-temporal variations in surface ozone over Ushuaia and the Antarctic region:

observations from in situ measurements, satellite data, and global models. Environ Sci Pollut Res, 25: 2194-2210, doi: 10.1007/s11356-017-0521-1.

Neff W, Helmig D, Grachev A, et al. 2008. A study of boundary layer behavior associated with high NO concentrations at the South Pole using a minisodar, tethered balloon and sonic anemometer. Atmos Environ, 42: 2762-2779, doi: 10.1016/j.atmosenv.2007.01.033.

Oltmans S J, Johnson B J, Helmig D. 2008. Episodes of high surface-ozone amounts at South Pole during summer and their impact on the long-term ozone variation. Atmos Environ, 42: 2804-2816, doi: 10.1016/j.atmosenv.2007.01.020.

Riedel K. 2005. Tropospheric ozone depletion events and air mass origin at Arrival Heights (Antarctica). Individual Project, Graduate Certificate in Antarctic Studies 2004/2005, February 2005 (Supervisor: Karin Kreher). https://pdfs.semanticscholar.org/1572/54f879f233336ef3c135a454c9b7ea70b646.pdf.

Schultz M G, Akimoto H, Bottenheim J, et al. 2015. The global atmosphere watch reactive gases measurement network. Elementa-Sci Anthrop, 3: 000067, doi: 10.12952/journal.elementa.000067.

Spicer C W, Plastridge R A, Foster K L, et al. 2002. Molecular halogens before and during ozone depletion events in the Arctic at polar sunrise: concentrations and sources. Atmos Environ, 36: 2721-2731, doi: 10.1016/S1352-2310(02)00125-5.

Stein A F, Draxler R R, Rolph G D, et al. 2015. NOAA's HYSPLIT atmospheric transport and dispersion modeling system. B Am Meteorol Soc, 96: 2059-2077, doi: 10.1175/BAMS-D-14-00110.1.

Sudo K, Akimoto H. 2007. Global source attribution of tropospheric ozone: Long-range transport from various source regions. J Geophys. Res, 112: D12302, doi: 10.1029/2006JD007992.

Tarasick D W, Bottenheim J W. 2002. Surface ozone during depletion episodes in the Arctic and Antarctic from historical ozonesonde records. Atmos Chem Phys, 2: 197-205, doi: 10.5194/acp-2-197-2002.

Tarasick D W, Carey-Smith T K, Hocking W K, et al. 2019. Quantifying stratosphere-troposphere transport of ozone using balloon-borne ozonesondes, radar windprofilers and trajectory models. Atmos Environ, 198: 496-509, doi: 10.1016/j.atmosenv.2018.10.040.

Wang Y T, Bian L G, Ma Y F, et al. 2011. Surface ozone monitoring and background characteristics at Zhongshan Station over Antarctica. Chin Sci Bull, 56(10): 1011-1019, doi: 10.1007/s11434-011-4406-2.